Prediction of Gas Tungsten Arc Welding Properties in Mixtures of Argon and Hydrogen

John J. Lowke, Richard Morrow, Jawad Haidar, and Anthony B. Murphy

***Abstract*—A theory of gas tungsten arc welding (GTAW) arcs that treats the tungsten electrode, the arc, and the workpiece as a unified system has been applied to make predictions in two dimensions of the temperature distributions in the arc, the tungsten cathode, and the workpiece, for any given arc current and gas mixture. Predictions of arc temperatures, radii, and voltages are compared for argon and mixtures of argon and hydrogen. It is found that arcs in gas mixtures containing hydrogen are more constricted and have a higher maximum temperature and arc voltage than arcs in pure argon. The addition of hydrogen also significantly increases the volume of molten material in the weld pool due to the higher thermal conductivity of argon–hydrogen mixtures at temperatures at which molecules of hydrogen dissociate. Predictions are also compared for workpieces of steel and aluminum. The volume of molten material is very much less for aluminum, despite its lower melting point, because of the higher thermal conductivity of aluminum. Predicted arc voltages as a function of current for a mixture of 10% hydrogen in argon are in good agreement with experimental results.**

***Index Terms*—Arc, argon, hydrogen, tungsten, welding.**

I. Introduction

IT IS well known in welding technology that weld properties are a function of the gas mixture used for the arc, and many different gas mixtures are in use for different applications. However, the effects of gas properties on the welding characteristics are not understood, and it has not been possible to make quantitative predictions of the effects of altering the gas composition.

In the present paper, we report progress made toward these ends. It is now possible to calculate the material properties of any specified gas mixture theoretically [1]. It is also possible to calculate, to a fair approximation, the steady-state temperature profiles for the arc plasma, and also the electrode and workpiece, for gas tungsten arc welding (GTAW) [2], [3]. Predictions for gas metal arc welding (GMAW) are much more complex because metal droplets are continually being formed, and the arc is never really in a steady state. Furthermore, for GMAW, the cathode is generally not a thermionic emitter, and account needs to be taken of the physical processes producing the electron current.

We have made calculations for GTAW to compare results for pure argon and mixtures of argon and up to 10% hydrogen by mole fraction. In arc welding, mixtures of only a few percent of hydrogen are ever used because of problems of porosity in welds and the possibility of hydrogen embrittlement with high percentages of hydrogen. Nevertheless, the calculations serve to illustrate major changes that occur when hydrogen is added, namely, an increase in the degree of constriction of the arc, the arc voltage, and the arc temperature. Results are given for both steel and aluminum as workpieces, as there has been recent interest in using high-current GTAW for both ferrous and nonferrous materials [4]. The calculations show the effects of the markedly different thermal conductivities of these metals.

The method of calculation assumes that the space-charge sheath at the electrodes is small and can be omitted [3], [5]. No assumption is made as to the current density distribution at the cathode as values of current density are derived for the whole arc–electrode region from the current continuity equation [6], [7]. Values of the electrical conductivity for mesh intervals next to the cathode are determined by solving the charge continuity equation using the ambipolar diffusion approximation [8]. Ionization within the sheath due to the electric field is omitted, and charge densities at the interface between the plasma and sheath region are taken at the equilibrium plasma value. The charge density at the cathode surface is calculated from the theoretical current from thermionic emission. The neglect of space-charge effects in the sheath region is supported in that the derived voltages between electrodes are in fair agreement with experimental results. There are other authors who believe that the space-charge region is very significant, even for thermionic cathodes [9], [10].

Significant energy exchanges need to be taken into account in the energy balance equation at the surfaces of the electrodes. There is a strong cooling effect on the tungsten due to electrons leaving the electrode overcoming the surface work function, and at the anode, where electrons enter the electrode, there is a corresponding heating effect. If the derived current density at the cathode surface is less than the thermionic current density corresponding to the local temperature, the difference must be due to ion current, which will give an additional heating effect to the cathode.

II. Material Functions

Input material functions required for the calculations include the thermal and electrical conductivity and the specific heat as functions of temperature. These material functions are calculated for an equilibrium plasma composition using the

Manuscript received October 21, 1996; revised December 2, 1997. This work was supported by the Cooperative Research Centre for Materials Joining and Welding—Australia.

The authors are with the CSIRO Division of Telecommunications and Industrial Physics, Sydney, NSW 2070, Australia.

Publisher Item Identifier S 0093-3813(97)07240-8.

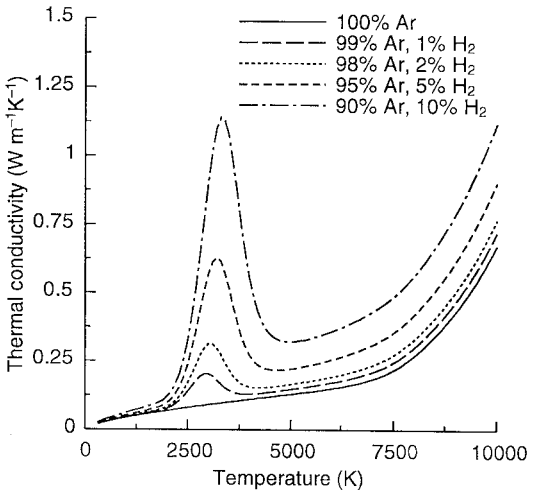

Fig. 1. Calculated values of thermal conductivity as a function of temperature for various mixtures of argon and hydrogen by mole.

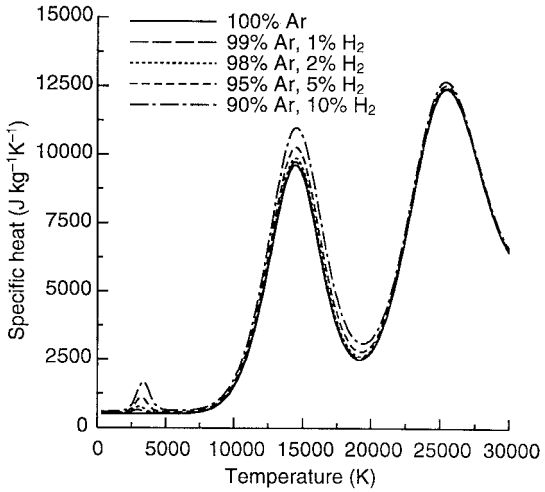

Fig. 2. Calculated values of specific heat as a function of temperature for various mixtures of argon and hydrogen by mole.

methods of Murphy and Arundell [1] and Gordon and McBride [11]. In the calculations, we have assumed that the fraction of hydrogen and argon is constant throughout the calculation domain. Demixing effects occur [12], [13], but influences on the heat fluxes for similar mixtures of argon and nitrogen are less than 10% [14]. However, demixing effects may be much larger for mixtures with hydrogen instead of nitrogen because the maximum in the thermal conductivity, which occurs at the temperatures for molecular dissociation, is much larger for hydrogen than for nitrogen.

The principal effect of adding small quantities of hydrogen to argon is on the thermal conductivity. Calculated values are shown in Fig. 1, where it is seen that the thermal conductivity at temperatures around 3000 K is increased by more than a factor of 10 if 10% hydrogen is added to argon. This increased thermal conductivity is caused by the dissociation of hydrogen molecules. Temperatures around 3000 K are critical because they are near the melting point of metals such as steel, and heat conduction from the arc plasma to the steel is enhanced by the hydrogen.

Figs. 2 and 3 show calculated values of the specific heat and electrical conductivity, respectively, as a function of temperature for various percentages of hydrogen in argon. The effect of adding hydrogen on material functions other than thermal conductivity is small, although the specific heat is increased about a factor of 3 at about 3000 K.

III. Theoretical Method and Basic Equations

We have used the method of Lowke *et al.* [3] to calculate the temperature profiles of the arc plasma, the tungsten electrode, and the workpiece as an integrated system. Basically, the four equations for conservation of mass, axial momentum, radial momentum, and energy are solved to obtain the temperature, axial velocity, radial velocity, and pressure, all in two dimensions, for the plasma–electrode system. In addition, the magnetic field is calculated in order to take account of the magnetic pinch forces that induce the plasma flow, and effects of thermionic cooling and heating and ion heating are included at the electrode surfaces. The electrode electrical resistivities and thermal conductivities are required as a function of temperature.

The plasma is assumed to be in local thermodynamic equilibrium, the flow is assumed to be laminar, and demixing is neglected. The equations of conservation of mass, enthalpy, radial momentum, and axial momentum are, respectively

$$\frac{1}{r}\frac{\partial}{\partial r}(r\rho v_r)+\frac{\partial}{\partial z}(\rho v_z) = 0 \tag{1}$$

$$\frac{\partial}{\partial r}(\rho v_r h)+\frac{\partial}{\partial z}(\rho v_z h) = \frac{1}{r}\frac{\partial}{\partial r}\left(\frac{r\kappa}{c_p}\frac{\partial h}{\partial r}\right)+\frac{\partial}{\partial z}\left(\frac{\kappa}{c_p}\frac{\partial h}{\partial z}\right)+\frac{j_r^2+j_z^2}{\sigma}-U \tag{2}$$

$$\frac{1}{r}\frac{\partial}{\partial r}(r\rho v_r^2)+\frac{\partial}{\partial z}(\rho v_r v_z) = -\frac{\partial P}{\partial r}-j_z B_\theta+\frac{1}{r}\frac{\partial}{\partial r}\left(2r\eta\frac{\partial v_r}{\partial r}\right)+\frac{\partial}{\partial z}\left(\eta\frac{\partial v_z}{\partial r}+\frac{\eta\partial v_r}{\partial z}\right)-2\eta\frac{v_r}{r^2} \tag{3}$$

$$\frac{1}{r}\frac{\partial}{\partial r}(r\rho v_z v_r)+\frac{\partial}{\partial z}(\rho v_z^2) = -\frac{\partial P}{\partial z}+j_r B_\theta+\frac{\partial}{\partial z}\left(2\eta\frac{\partial v_z}{\partial r}\right)+\frac{1}{r}\frac{\partial}{\partial r}\left(\frac{r\eta\partial v_z}{\partial r}+\frac{r\eta\partial v_r}{\partial z}\right)+\rho g. \tag{4}$$

Equations (1)–(4) define the enthalpy h, the pressure P, and the axial and radial velocities v_z and v_r of the arc column as a function of the radial and axial coordinates r and z. The material functions are the thermal conductivity κ, the electrical conductivity σ, the specific heat c_p, the density ρ, the radiation emission coefficient U, and the viscosity η, all of which are required inputs as a function of temperature for the ambient pressure of the arc; g is the acceleration due to gravity. The current densities j_z and j_r are evaluated from Ohm's law, $\boldsymbol{j}=\sigma\boldsymbol{E}$, where the electric field, $\boldsymbol{E}$, is obtained from $\boldsymbol{E}=-\nabla\phi$. The electric potential ϕ is obtained from a

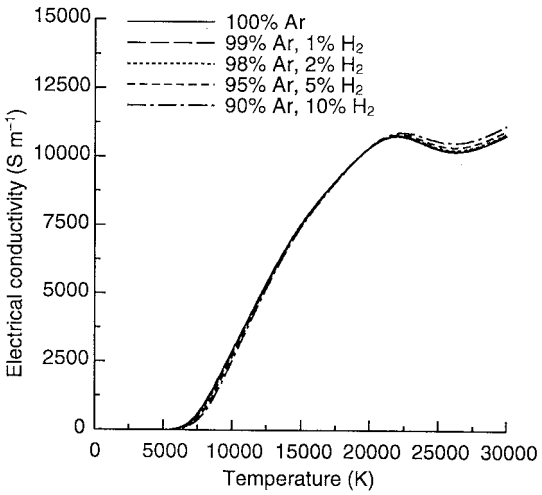

Fig. 3. Calculated values of electrical conductivity as a function of temperature for various mixtures of argon and hydrogen by mole.

solution of the current continuity equation, i.e.,

$$\nabla \cdot (\sigma \nabla \phi) = 0. \tag{5}$$

The magnetic field B_θ is obtained from Maxwell's equation: $(1/r)\partial(rB_\theta)/\partial r = \mu_0 j_z$, where μ_0 is the permeability of free space.

The integration region is a cylinder 4.3 cm long with a radius of 3.5 cm, containing a cylindrical thoriated tungsten cathode 3.5 cm long and diameter 3.2 mm with a conical tip with an included angle of 60°. The cathode conical region has a flat tip of radius 0.2 mm. The boundary conditions of (1)–(4) for the external boundaries are that the temperature is 300 K and there is an imposed gas flow of 166 cm^3/s around the cathode through a radius at the cathode entrance of 0.66 cm. Flow boundary conditions at other external boundaries maintain the continuity of flow [7]. Along the axis of the integration region, temperature gradients, axial velocity gradients, and the radial velocity are set to zero. The arc pressure is taken as 1 bar at the point on the entrance plane at the outer boundary of the integration region. The electric potential is set to zero at the base of the workpiece. The potential is evaluated for the integration region from the solution of the current continuity (5) for a given total current [7].

The integration region over which solutions of (1)–(5) are obtained contains electrode and arc regions. Material functions appropriate to the electrodes and the plasma are used for each region. In the solid electrodes, there is no convection, and convective effects are also omitted in the liquid weld pool, so (1), (3), and (4) are not used in these regions. The radiation emission coefficient U for the plasma was taken for visible radiation only [15], neglecting self-absorption effects.

Calculations at grid points on the electrode surfaces need to include special processes occurring at the surfaces. We account for energy losses by thermal radiation from the hot electrode, cooling or heating by the electrons leaving or entering the solid, and heating by ion bombardment. Heating of the electrodes by radiation from the arc is neglected. For the cathode, the additional energy flux F to the electrodes is

$$F = -\varepsilon a T^4 - j\psi + j_i V_i; \tag{6}$$

ε is the emissivity of the surface, T is the surface temperature, ψ is the work function, j_i is the ion current density, a is the Stefan–Boltzmann constant, and V_i is the ionization potential of the plasma. The term in ψ represents the loss in energy from electrons leaving the cathode and overcoming the work function potential. The ion current density j_i is assumed to be $j - j_R$ at the cathode surface, where j is the current density at the cathode surface obtained from the current continuity equation, and j_R is the Richardson current density due to thermionic emission of electrons from the surface; $j_R = AT^2 \exp(-\psi e/k_B T)$; e is the electronic charge, k_B is Boltzmann's constant, and A is the thermionic emission constant for the surface of the cathode. If j_R is greater than j, we take j_i to be zero. If j is greater than j_R, we assume that the additional electrons originate in the plasma by back diffusion. At the anode surface, we change the sign of the term in $j\psi$ of (6) to be positive since electrons heat the anode due to the work function potential. We assume that there is no ion current, and hence no ion heating at the anode.

The value of the emissivity for the thoriated tungsten cathode was approximated as 0.3, independent of temperature [16]. Workpiece temperatures are much lower than the cathode, and thus for the workpiece, the thermal radiation emission term of (6) is insignificant.

The sheath regions near the electrodes are treated as in the investigation of [3]. The computations typically use 70 × 70 grid points to span the whole arc–electrode region using a nonuniform mesh. The mesh size at the electrodes is 0.005 cm, which is approximately the mean free path of the electrons. Results are insensitive to the size of the mesh at the cathode, as in the investigation of [3].

For mesh cells adjacent to the anode surface, the electrical conductivity is taken simply as the equilibrium plasma value for the temperature on the plasma side of the cell. The results of Figs. 4–7, discussed later, are also insensitive to the size of the mesh at the anode; for example, in Fig. 4, the predicted temperature of the anode at a radius of 0.44 cm at the edge of the molten region changes from 1790 to 1820 K, with a change in mesh size at the anode of 0.005 to 0.02 cm. However, the current density distribution over the anode is, to some extent, dependent on the mesh size. The current density at the center of the anode changes from 980 $A \cdot cm^{-2}$ with a mesh size of 0.005 cm to a current density of 640 $A \cdot cm^{-2}$ with a mesh size of 0.02 cm. Convergence is generally obtained for each arc current in about 200 iterations, taking about 5 min on a Silicon Graphics Challenge L computer.

IV. Results

Fig. 4 shows calculated results for a 200 A arc in pure argon with a gap between the tungsten cathode and a steel workpiece of 3 mm. The calculated arc and tungsten temperatures are in good agreement with experimental values for a similar system, where the maximum arc temperature was 23 000 K [17] and the temperature at the cathode tip was 3800 K [18].

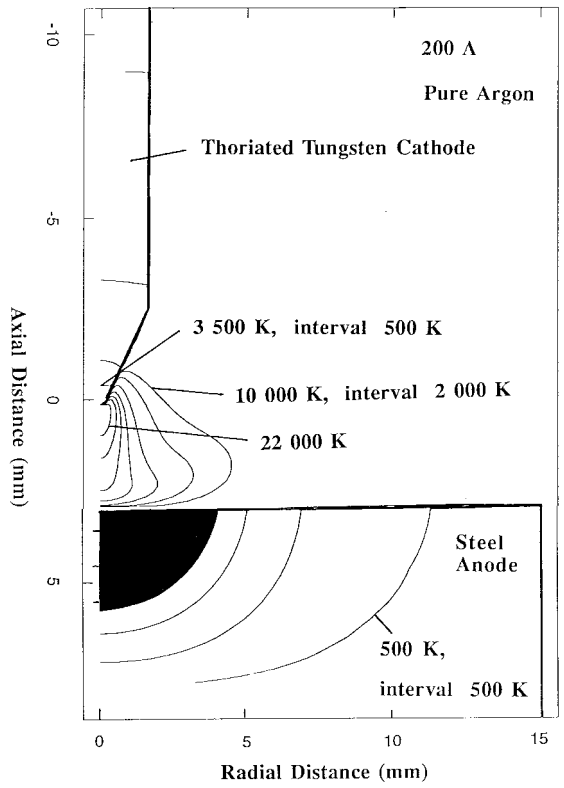

Fig. 4. Calculated values of temperature distributions for a 200 A arc in pure argon, with a steel workpiece.

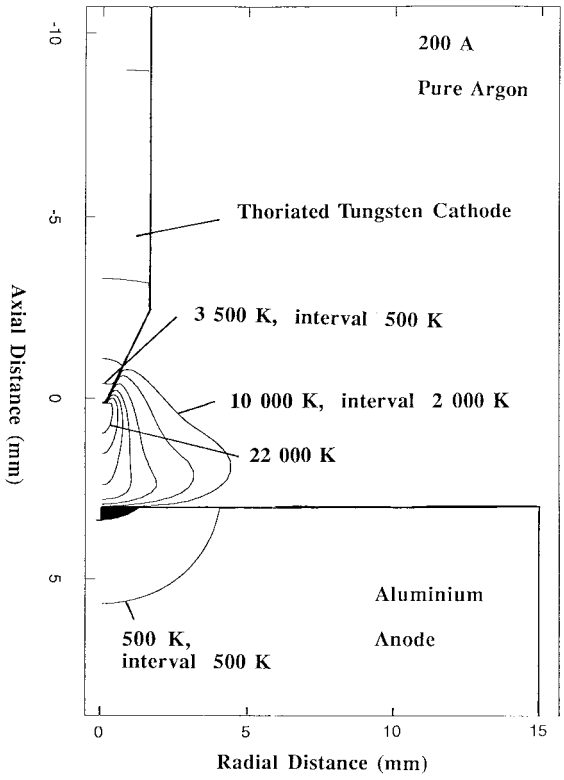

Fig. 6. Calculated values of temperature distributions for a 200 A arc in pure argon, with an aluminum workpiece.

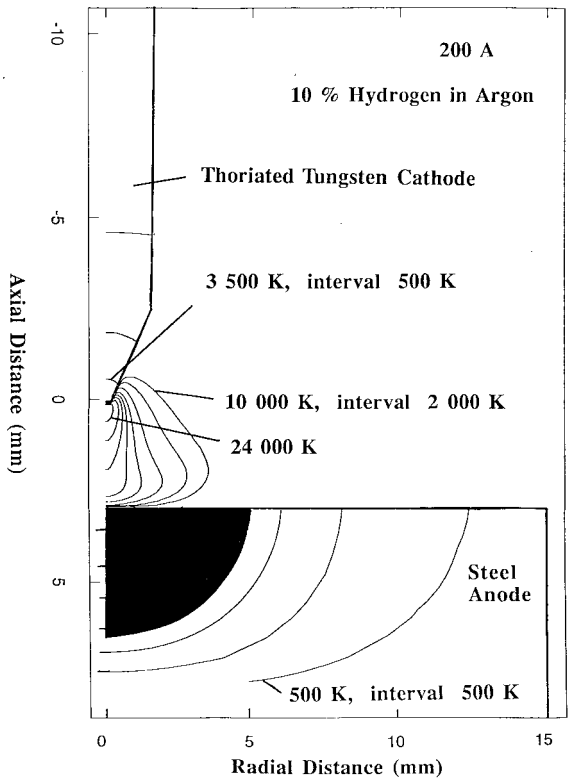

Fig. 5. Calculated values of temperature distributions for a 200 A arc in argon and 10% hydrogen by mole, with a steel workpiece.

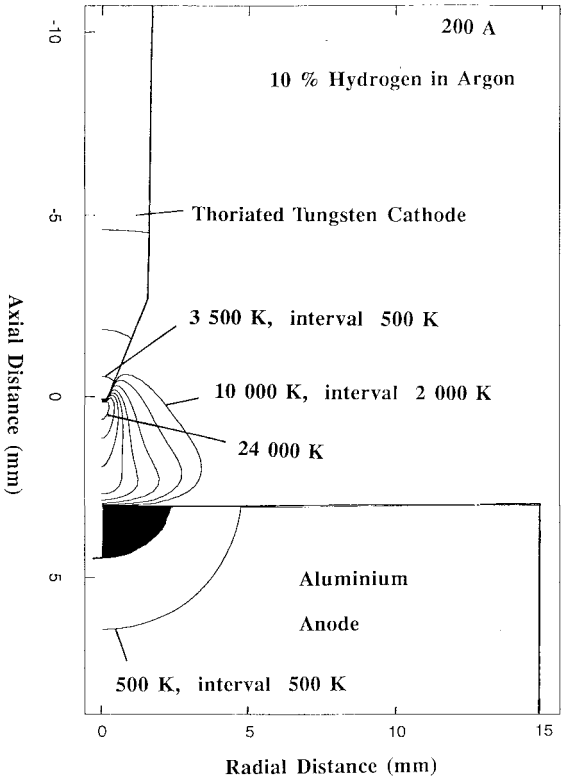

Fig. 7. Calculated temperature profiles for a 200 A arc in argon and 10% hydrogen by mole, with an aluminum workpiece.

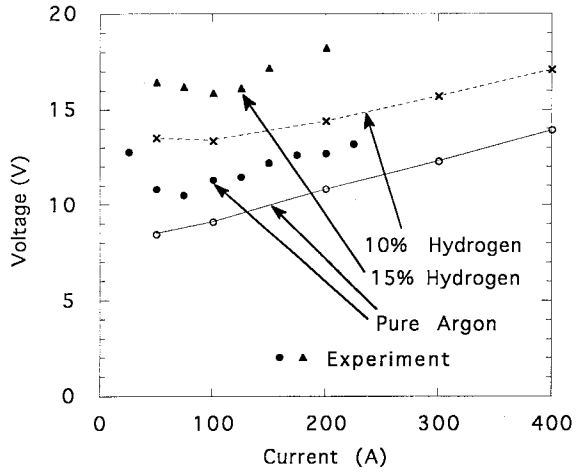

Fig. 8. Comparison of predicted and calculated arc voltages as a function of current.

The predicted molten region in the steel is shown in black. This region is simply the region of the metal calculated to be above its melting point, with no account taken of the change in material functions from solid to liquid, convection in the weld pool, or the latent heat of fusion of the metal. Nevertheless, it is considered that the region in black gives an indication of the degree of melting that is to be expected in the workpiece.

Fig. 5 shows predicted curves for a similar system, but with 10% hydrogen in the argon. The volume of molten metal is significantly larger than for the pure argon case of Fig. 4 as a consequence of the higher thermal conductivity of the arc plasma. In addition, the central arc temperature is higher, being above 24 000 K, and the arc is more constricted.

Fig. 6 shows calculations for pure argon, but with aluminum instead of steel as the workpiece. Arc plasma and cathode temperature predictions are little changed from those of Fig. 4 with a steel workpiece. However, the predicted volume of molten material is very much reduced, even though the melting point of aluminum, 930 K, is very much less than that of steel, which is 1800 K. The results illustrate the very strong effect of the high thermal conductivity of aluminum in conducting heat away, thus reducing the volume of molten metal. Fig. 7 shows the effect of 10% hydrogen in the argon with an aluminum workpiece. It is seen that the predicted volume of the molten aluminum is significantly increased.

Fig. 8 shows predicted arc voltages as a function of arc current compared with the experimental results of Hooijmans [19]. The experimental results are for a 15% mixture of hydrogen and argon, whereas the theoretical results are for 10% hydrogen. The experimental voltages are slightly higher than the theoretical results, consistent with what would be expected for a higher percentage of hydrogen. However, it is noted that there are differences between theory and experiment for pure argon. Such differences are to be expected due to our neglect of the space-charge sheath, and also due to inaccuracies in the radiation emission coefficient and our neglect of the self-absorption of radiation.

The predicted maximum velocities of the axial flow of plasma range, for pure argon, from 50 m/s at 50 A to 740 m/s at 400 A. With the addition of 10% of hydrogen, these values increase due to the higher magnetic pinch pressure of the more constricted arc to be 90 m/s at 50 A and 900 m/s at 400 A.

V. Conclusion

Recently developed computational methods have been used to calculate properties of gas tungsten arc welding, where the electrodes, arc, and workpiece are treated together in a unified system. The properties of different gas mixtures of the welding gas can be calculated and quantitative predictions made of effects of each gaseous component on the temperature distribution in the electrodes. In the present paper, predictions are made for various mixtures of argon and hydrogen. The effect of the addition of hydrogen is 1) to make the arc more constricted, 2) to increase the arc voltage, 3) to increase the arc temperature, and 4) to increase the volume of the molten material of the workpiece for a given arc current.

Acknowledgment

The authors are indebted to B. Canak for assistance with the calculations. They are also indebted for discussions with their colleagues, N. Ahmed and L. Jarvis, of the CSIRO Division of Manufacturing Technology, Adelaide, Australia.

References

[1] A. B. Murphy and C. J. Arundell, "Transport coefficients of argon, nitrogen, oxygen, argon-nitrogen, and argon-oxygen plasmas," *Plasma Chem. Plasma Process.*, vol. 14, pp. 451–490, 1994.

[2] P. Zhu, J. J. Lowke, R. Morrow, and J. Haidar, "Prediction of anode temperatures of free burning arcs," *J. Phys. D, Appl. Phys.*, vol. 25, pp. 1369–1376, 1995.

[3] J. J. Lowke, R. Morrow, and J. Haidar, "A simplified theory of arcs and their electrodes," in *Proc. 12th Int. Symp. Plasma Chem.*, Minneapolis, MN, 1995, pp. 1449–1455; also, *J. Phys. D, Appl. Phys.*, pp. 2033–2042, 1997.

[4] N. U. Ahmed, B. L. Jarvis, and D. M. Viano, "High current gas tungsten arc welding," in *Proc. 42nd Nat. Welding Conf.*, WTIA, Melbourne, Australia, 1994, vol. 2, paper 26.

[5] J. J. Lowke and J. C. Quartel, "Use of transport coefficients to calculate properties of electrode sheaths of electric arcs," *Aust. J. Phys.*, vol. 50, pp. 539–552, 1997; also in *Proc. 11th Int. Conf. Gas Discharges Appl.*, Tokyo, Japan, 1995, p. 90.

[6] J. J. Lowke, P. Kovitya, and H. P. Schmidt, "Theory of free burning arc columns including the influence of the cathode," *J. Phys. D, Appl. Phys.*, vol. 25, pp. 1600–1606, 1992.

[7] P. Zhu, J. J. Lowke, and R. Morrow, "A unified theory of free burning arcs, cathode sheaths and cathodes," *J. Phys. D, Appl. Phys.*, vol. 25, pp. 1221–1230, 1992.

[8] R. Morrow and J. J. Lowke, "A one-dimensional theory for the electrode sheaths of electric arcs," *J. Phys. D, Appl. Phys.*, vol. 26, pp. 634–642, 1993.

[9] X. Zhou and J. Heberlein, "Analysis of the arc-cathode interaction of free burning arcs," *Plasma Sources Sci. Technol.*, vol. 3, p. 564, 1994.

[10] M. S. Benilov and A. Marotta, "A model of the cathode region of atmospheric pressure arcs," *J. Phys. D, Appl. Phys.*, vol. 28, p. 1869, 1995.

[11] S. Gordon and B. J. McBride, "Computer program for calculation of complex chemical equilibrium compositions," NASA Special Publ. SP-273, 1971.

[12] A. B. Murphy, "Modeling and diagnostics of plasma chemical processes in mixed-gas arcs," *Pure Appl. Chem.*, vol. 68, pp. 1137–1142, 1996.

[13] S. C. Snyder, A. B. Murphy, D. L. Hofeldt, and L. D. Reynolds, "Diffusion of atomic hydrogen in an atmospheric-pressure free-burning arc discharge," *Phys. Rev. E*, vol. 52, pp. 2999–3009, 1995.

[14] A. B. Murphy, "The influence of demixing on the properties of a free burning arc," *Appl. Phys. Lett.*, vol. 69, pp. 328–330, 1996.

[15] D. L. Evans and R. S. Tankin "Measurement of emission and absorption of radiation by an argon plasma," *Phys. Fluids*, vol. 10, p. 1137, 1967.
[16] R. C. Weast, Ed., *CRC Handbook of Chemistry and Physics*, 70th ed. Boca Raton, FL: CRC Press, 1989.
[17] G. N. Haddad and A. J. D. Farmer, "Temperature determinations in a free burning arc," *J. Phys. D, Appl. Phys.*, vol. 17, p. 1189, 1984.
[18] J. Haidar and A. J. D. Farmer "A method for the measurement of the cathode surface temperature for a high current free burning arc," *Rev. Sci. Instrum.*, vol. 64, p. 542, 1993.
[19] J. W. Hooijmans, "Hydrogen absorption in iron and steel during gas tungsten arc welding," thesis, Delft Univ. Technol., the Netherlands, 1994.

John J. Lowke was born in Tanunda, South Australia, on April 3, 1934. He received the science degree from the University of Adelaide, South Australia, with first class honors in physics in 1956, and received the Ph.D. degree in physics in 1963.

From 1964 to 1975, he worked as a Senior Physicist, and then a Fellow Scientist, at the Westinghouse Research Laboratories, Pittsburgh, PA. From 1976 to 1980, he was a Senior Lecturer, and then Reader, in the Department of Electrical Engineering, University of Sydney, Australia. From 1980 to 1988, he was Chief of the CSIRO Division of Applied Physics, Sydney, Australia, and since then, he has continued at CSIRO as a Chief Research Scientist. His major interests are in the theory of electrical discharges in gases, including circuit breakers, arc lamps, gas lasers, electrostatic precipitators, and arc welding.

Richard Morrow received the B.Sc. degree from the University of Adelaide, South Australia, in 1966, and the Ph.D. degree (on the propagation of Alfen waves) from Flinders University, South Australia, in 1971.

In 1971, he joined Liverpool University, U.K., , as a Postdoctoral Fellow, and in 1972, joined the Electricity Council Research Centre, Capenhurst, U.K., as a Research Officer, working on the use of radio-frequency power in industry. He then joined the CSIRO Division of Applied Physics, Sydney, Australia, in 1975, where he is a Principal Research Scientist. His current research interests include the modeling of space-charge-dominated discharges such as electrical coronas, lasers, and arc sheaths, and the development of accurate numerical methods for such calculations.

Jawad Haidar was born in Lebanon in 1961. He received the B.Sc. degree in physics from the Lebanese University, Beyrouth, and the DEA and the Doctorate degrees in gas and plasma physics from the University of Paris VI, France, in 1983, 1986, and 1989, respectively.

He joined CSIRO, Sydney, Australia, in 1990, and since then, he has been involved in experimental and theoretical work in the field of gas discharges. His research interests include high-pressure arcs, electrode phenomena, arc welding, numerical modeling, computational fluid dynamics, and dielectric barrier discharges.

Anthony B. Murphy, for a photograph and biography, see this issue, p. 814.